

The luminosity function of high-redshift QSOs

Fabio Fontanot^{1,2}, Stefano Cristiani³, Pierluigi Monaco², Eros Vanzella³,
Mario Nonino³, W. Niel Brandt⁴, Andrea Grazian⁵, Jirong Mao⁶

Abstract. We measure the luminosity function of QSOs in the redshift range $3.5 < z < 5.2$ for the absolute magnitude interval $-21 < M_{145} < -28$. Suitable criteria are defined to select faint QSOs in the GOODS fields, checking their effectiveness and completeness in detail. The confirmed sample of faint QSOs is compared with a brighter one derived from the SDSS. Using a Monte-Carlo technique we estimate the properties of the luminosity function. Our results show that models based on pure density evolution show better agreement with observation than models based on pure luminosity evolution, even if a different break magnitude with respect to $z \sim 2.1$ is required at $3.5 < z < 5.2$. According to our modeling a faint-end slope steeper than low-redshift observations is required to reproduce the data, moreover models with a steep bright-end slope score a higher probability than models with a bright-end flattening. Determining the faint-end of the luminosity function at these redshifts provides important constraints on models of the joint evolution of galaxies and AGNs.

1. Introduction

In recent years evidence has grown that QSOs represent a necessary phase of galactic evolution. Several models for a joint evolution of galaxies and QSOs (see i.e. Granato et al. 2004; Hopkins et al. 2005; Bower et al. 2006; Croton et al. 2006; Menci et al. 2006; Monaco, Fontanot & Taffoni 2006) are able to reproduce the properties of present-day elliptical galaxies by assuming that their vigorous star formation at high redshift is quenched by the feedback (i.e. galactic winds). This process is likely triggered by the QSO activity fed by the accretion of matter onto a supermassive black hole (SMBH) at the center of the galaxy itself (see also Monaco & Fontanot 2005). In this framework the detailed determination of properties of high redshift QSOs is fundamental in understanding the phenomena driving galaxy formation. In particular the study of the Lumi-

¹Max-Planck-Institut for Astronomy, Koenigstuhl 17, 69117 Heidelberg, Germany

²Dipartimento di Astronomia dell'Università, Via Tiepolo 11, I-34131 Trieste, Italy

³INAF-Osservatorio Astronomico, Via Tiepolo 11, I-34131 Trieste, Italy

⁴Department of Astronomy and Astrophysics, Pennsylvania State University, 525 Davey Lab, University Park, PA 16802

⁵INAF-Osservatorio Astronomico di Roma, via Frascati 33, I-00040 Monteporzio, Italy

⁶SISSA, via Beirut 2-4, I-34014 Trieste, Italy

osity Function (LF) provides strong constraints for the physical mechanisms involved.

A great improvement in the determination of this statistical quantity has been achieved thanks to the large amount of data coming from major observational programs such as the *Two Degree Field QSO Redshift Survey* (2QZ, Croom et al. 2004) and in particular the third edition of the *Sloan Digital Sky Survey* Quasar Catalog (DR3QSO, Schneider et al. 2005). However, at high redshift the SDSS is sensitive only to the brightest QSOs; on the other hand the faint-end of the high- z QSO LF plays a key role for comparing different predictions of the formation and evolution of galaxies. In this work we estimate the QSO LF and space density at $3.5 < z < 5.2$, down to $M_{145} < -21$.

2. The database

We combine a bright quasar sample extracted from the DR3QSO, with a faint sample recently determined by Cristiani et al. (2004) and Fontanot et al. (2006a) using optical and X-ray observations in the framework of the *Great Observatories Origins Deep Survey* (GOODS) project. The selection of QSO candidates at different redshift in SDSS field has been carried out using color criteria: Richards et al. (2002) presented the updated version of these criteria and in the following we use their eq. 6 and 7 as SDSS selection criteria to select a high- z QSOs sample out of the DR3QSO. The DR3QSO is a sample with an incomplete spectroscopic follow-up. We consider those objects in the SDSS photometric catalogue that satisfy the SDSS criteria and we compare them to the corresponding SDSS spectroscopic catalogue: this way, we estimate that $\sim 21\%$ of the high- z QSO candidates have a spectrum.

In order to select a sample of faint QSOs from the GOODS catalogues we consider the optical catalogues obtained using the ACS (Advanced Camera for Surveys) in the B_{445} , V_{660} , i_{775} , z_{850} bands (Giavalisco et al. 2004a). The catalogues are z -band-based with magnitude limits in the four bands are respectively 27.50, 27.25, 27.00, 26.5. The selection of the QSO candidates is carried out in the magnitude interval $22.25 < z_{850} < 25.25$. Expected QSO colors in different photometric systems are estimated as a function of redshift using a template spectrum of Cristiani & Vio (1990) for the QSO spectral energy distribution (SED) convolved with a model of the intergalactic medium (IGM) absorption. Four optical criteria has been tailored to select QSOs in the redshift interval $3.5 \lesssim z \lesssim 5.2$ as described in Cristiani et al. (2004) and Fontanot et al. (2006a). These color selection criteria are known to select a broad range of high- z AGN, not limited to broad-lined (type-1) QSOs, and are less stringent than those typically used to identify high- z galaxies (e.g. Giavalisco et al. 2004b). In order to reduce the number of The optically selected candidates we match them with X-ray Chandra observations in the HDF-N and CDF-S (for 2 Ms and 1 Ms, respectively Alexander et al. 2003; Giacconi et al. 2002), within an error radius corresponding to the 3σ X-ray positional uncertainty. The X-ray completeness limits over $\approx 90\%$ of the area of the GOODS fields are similar, with flux limits (S/N= 5) of $\approx 1.7 \times 10^{-16}$ erg cm $^{-2}$ s $^{-1}$ (0.5–2.0 keV) and $\approx 1.2 \times 10^{-15}$ erg cm $^{-2}$ s $^{-1}$ (2–8 keV) in the HDF-N field and $\approx 2.2 \times 10^{-16}$ erg cm $^{-2}$ s $^{-1}$ (0.5–2.0 keV) and $\approx 1.5 \times 10^{-15}$ erg cm $^{-2}$ s $^{-1}$

(2–8 keV) in the CDF-S field. The sensitivity at the aim point is about 2 and 4 times better for the CDF-S and HDF-N, respectively. Given those flux limits, Type-1 QSOs with $M_{145} < -21$ are detectable up to $z \gtrsim 5.2$, up to an optical-to-X-ray flux ratio $\alpha_{ox} \gtrsim -1.7$. Recently Steffen et al. (2006) provide an estimate of α_{ox} statistics (their Table 5): at this optical luminosity they observed a mean value lower than this limit ($\alpha_{ox} = -1.408 \pm 0.165$). Conversely, any $z > 3.5$ source in the GOODS region detected in the X-rays must harbor an AGN ($L_x(0.5 - 2 \text{ keV}) \gtrsim 10^{43} \text{ erg s}^{-1}$). The final sample of QSO candidates consists of 16 candidates, 10 in CDF-S and 6 in HDF-N and it is presented in Fontanot et al. (2006a, their Table 1).

Spectroscopic information for all 16 candidates has been obtained (Vanzella et al. 2006; Cowie et al. 2004; Szokoly et al. 2004; Barger et al. 2003; Norman et al. 2002; Cristiani et al. 2000). Thirteen (5 in the HDF-N and 8 in CDF-S) candidates turn out to be *AGN*, with 8 QSOs at $z > 3.5$ (3 and 5), of which 2 (0 and 2) are identified as Type II. One object turns out to be a QSO with a redshift $z = 4.759$. In addition to the already known QSO at $z = 5.189$ (Barger et al. 2002), it brings to two the total number of objects in the redshift range $4 < z < 5.2$, where our selection criteria are expected to be most complete and reliable.

3. Estimating the luminosity function of high-*z* QSOs

In order to build up the high-*z* QSO LF from the joint analysis of GOODS and SDSS observations a Monte-Carlo technique is adopted. Mock QSO catalogues in GOODS and SDSS photometric systems are generated, starting from an assumed parameterization of the LF and they are compared to real catalogues using a χ^2 estimator to quantify the agreement between real data and the functional form of the LF. In order to clone the properties of high-*z* objects we define a QSO template library, tailored using high-quality SDSS QSO spectra at lower redshift. We choose the redshift interval $2.2 < z < 2.25$, for which the SDSS sample had the highest possible level of completeness and the continuum of the QSOs was sampled in the largest possible wavelength interval from the $Ly\alpha$ emission upward. The rest-frame spectrum of each selected object blueward of the $Ly\alpha$ line is estimated using the continuum fitting technique derived from Natali et al. (1998). The library is then used to compute the distribution of theoretical QSOs colors at increasing redshift in the SDSS and ACS photometric systems. In Fig. 1 (left panel) we show our results for the SDSS photometric system compared to the colors of observed QSOs in DR3QSO. The points refer to the colors of observed QSOs at different redshifts (red stars refer to objects with $3.5 < z < 4.0$; green squares to $4.0 < z < 5.2$; filled circles to $z > 5.2$; cyan dots to $z < 3.5$). The dotted line shows the projection of the SDSS selection criteria. The mean QSO color in our library is represented by the solid line. Dashed lines are 5% and 95% percentiles of color distribution in the template library (photometric errors are not accounted for). Similar results hold for the GOODS survey.

In order to estimate the QSO LF, the approach of La Franca & Cristiani (1997) is adopted. An LF of the form of a double power law is assumed, a pure luminosity evolution (PLE) or a pure density evolution (PDE) with a power

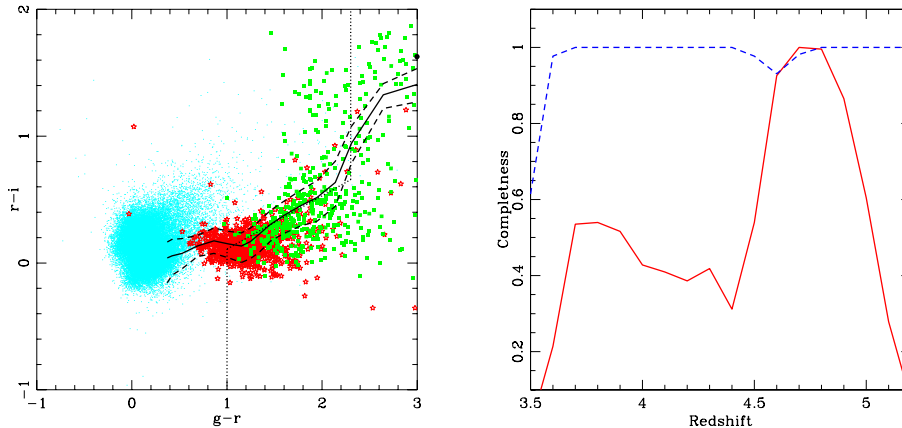


Figure 1. *Left panel:* Color diagrams for the confirmed QSOs in DR3QSO. *Right panel:* Completeness of selection criteria at various redshifts. The solid line refers to the SDSS selection criteria for SDSS sources. The dashed line refers to Cristiani et al. (2004) selection criteria in the GOODS fields.

law form and, alternatively, with an exponential form are adopted. Given a value for the break luminosity M^* , the slopes α and β of the double power law, the normalization Φ^* , and the redshift evolution parameter k_z , it is possible to calculate the expected number of objects from the LF up to a given magnitude in a given area of the sky. For each object a value of absolute M_{145} , a redshift and a template spectrum are extracted. We then use the template k-correction and colors at the corresponding redshift to simulate the apparent magnitudes in the SDSS and ACS photometric systems. The photometric errors in each band are estimated using SDSS and GOODS main photometric catalogues, and added to the simulated magnitudes. The corresponding color selection criteria are applied to the generated catalogues to obtain mock SDSS and GOODS QSO catalogues. In order to limit the statistical error multiple realizations are considered for each parameter set. The agreement between real and mock catalogues is evaluated using both a χ^2 statistic and a Kolmogorov-Smirnoff test. The best fit parameters for each model are estimated using a minimization technique. The results are collected in Fontanot et al. (2006a), Table 3 and the best-fitting model is shown in Fig. 2 (left panel).

4. Results

It is impossible to reproduce the observed QSO distribution with PLE models. PDE models show better agreement with observations, even if a luminosity evolution of the magnitude of the break, M_{145}^* , from $z = 2.1$ to $z = 3.5$ is required. Parameterizations assuming a relatively steep faint-end slope similar to the low- z estimate by Richards et al. (2005, SDSS combined to 2dF sample) score a higher probability with respect to those with a faint-end slope as flat as in Croom et al. (2004, 2dF sample). Models with a shallower slope of the bright-end of the LF (as suggested by Fan et al. 2003) are not able to reproduce

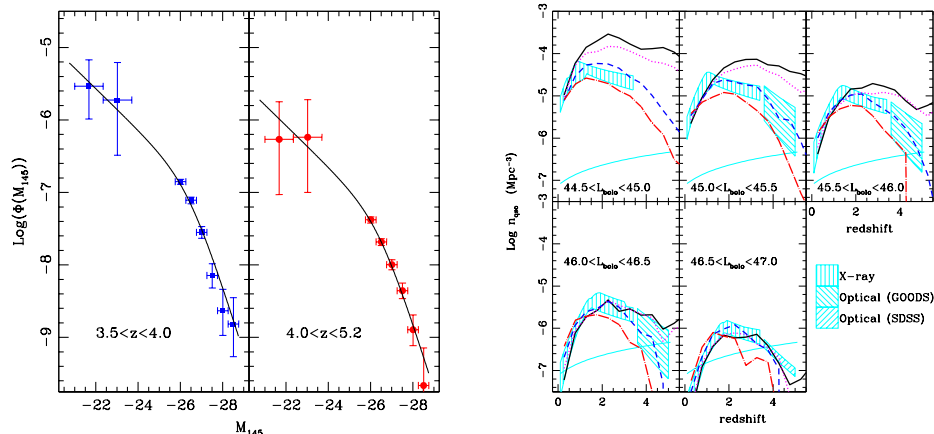


Figure 2. *Left panel:* analytical fit to the high- z QSO LF. The solid line shows, as a reference, the best fit model. The position of the filled symbols is obtained by multiplying the values of this model by the ratio between the number of observed sources and the number of simulated sources. La Franca & Cristiani (1997) demonstrated that this technique is less prone to evolutionary biases with respect to the conventional $\mathbf{1}/V_{\text{max}}$ technique. *Right panel:* Space density evolution of QSOs, compared to the predictions of MORGANA model (Monaco, Fontanot & Taffoni 2006; Fontanot et al. 2006b). The (black) solid line, the (magenta) dotted line, the (blue) dashed line and the (red) dot-dashed refer to different values of the σ_0 parameter (see text): **0**, **30**, **60** and **90** respectively (values are in Kms^{-1}).

the observed distributions: a bright-end slope as steep as in Croom et al. (2004) is required. This result is at variance with Richards et al. (2006).

In order to understand the origin of this discrepancy we focus our attention on the completeness of the samples selected using the GOODS and SDSS criteria. To obtain a robust estimate of this quantity we apply the selection criteria to our template library and analyze the fraction of QSOs recovered at various redshifts. The resulting completeness is shown in Figure 1 (right panel). As a comparison Richards et al. (2006) estimated the completeness of their criteria to be well above 90% in the whole range of redshift of interest. We check that this is related to the fact that the SDSS selection criteria are tailored on a QSO template spectra whose mean continuum slope $f_\nu \propto \nu^{-\gamma}$ is “bluer” ($\gamma = 0.5 \pm 0.3$ Fan et al. 1999) than the mean slope in our template library ($\gamma = 0.7 \pm 0.3$). The inferred completeness has a direct consequence on the shape and evolution of the estimated QSO LF. Assuming the Richards et al. (2006) completeness, the models with a shallow bright-end score higher probabilities with respect to models with a steep bright-end.

We use our best estimate for the LF to compute the QSO contribution to the UV background at redshift $3.5 < z < 5.2$, following the method outlined by Barger et al. (2003). We conclude that the QSO contribution is insufficient for ionizing the IGM at these redshifts.

When compared to physically motivated models, the present results show that to reproduce the observations it is necessary to suppress the formation/feeding

of low-mass BHs inside DMHs at high redshift. As a consequence the present estimate of the space density of high- z faint QSOs gives strong constraints to models of joint formation and evolution of galaxies and AGN. In fig. 1 (right panel) we compare the evolution of the QSO space density in bin of bolometric luminosity with the predictions of the MORGANA model (Monaco, Fontanot & Taffoni 2006, the detailed description of the model is beyond the scope of present proceedings and can be found in that paper). In Fontanot et al. (2006b) we propose that kinetic feedback is the key process responsible for the downsizing of the AGN population: in that paper we demonstrate that the velocity dispersion of cold clouds σ , due to turbulence induced by exploding SNe, scales with the star formation time-scale t_* as $\sigma = \sigma_0(t_*/1 \text{ Gyr})^{1/3}$; the normalization σ_0 regulates the level of turbulence, so that a high value ($\sim 50 \text{ km s}^{-1}$) induces significant mass loss from small star-forming bulges at high redshift. Different lines in fig. 1 (right panel) refer to model with different values for σ_0 (see caption for more details). It is evident from the figure that the space density evolution of high- z low-luminosity AGN is of fundamental importance to constrain this physical mechanism.

References

- Alexander, D.M., Bauer, F.E., Brandt, W.N. et al. 2003, AJ 126, 539
 Barger, A.J., Cowie, L.L., Brandt, W.N. et al. 2002, AJ 124, 1839
 Barger, A.J., Cowie, L.L., Capak, P. et al. 2003, ApJ 584, L61
 Bower, R. G., Benson, A. J., Malbon, R. et al. 2006, MNRAS, 659
 Cowie, L. L., Barger, A. J., Hu, E. M., Capak, P., & Songaila, A. 2004, AJ 127, 3137
 Cristiani, S., Vio R. 1990, A&A 227, 385
 Cristiani, S., Appenzeller, I. Arnouts, S. et al. 2000, A&A 359, 489
 Cristiani, S., Alexander, D.M., Bauer, F. et al. 2004, ApJ 600, L119
 Croom, S. M., Smith, R. J., Boyle, B. J., et al. 2004, MNRAS 349, 1397 (Cr4)
 Croton, D. J., Springel, V., White, S.D.M. et al. 2006, MNRAS 365, 11
 Fan, X., Strauss, M.A., Gunn, J.E. et al. 1999, ApJ 526, L57
 Fan, X., Strauss, M.A., Schneider, D.P., & Becker, R.H. 2003 AJ 125, 1649
 Fontanot F., Cristiani S., Monaco P., Nonino M., Vanzella E., Brandt W.N., Grazian A., Mao J. 2006, A&A in press (astro-ph/0608664)
 Fontanot F., Monaco, P., Cristiani, S., & Tozzi, P. 2006, MNRAS in press, (astro-ph/0609823)
 Giacconi, R., Zirm, A., Wang, J.X. et al. 2002, ApJS 139, 369
 Giavalisco, M., Ferguson, H.C., Koekemoer, A.M., et al. 2004a, ApJ 600, L93
 Giavalisco, Dickinson, M., Ferguson, H.C. et al. 2004b, ApJ 600, L103
 Granato, G. L., De Zotti, G., Silva, L., Bressan, A., & Danese, L. 2004, ApJ 600, 580
 La Franca, F., Cristiani, S. 1997, AJ 113, 1517
 Hopkins, P. F., Hernquist, L., Cox, T. J. et al. 2005, ApJ 630, 705
 Menci, N., Fontana, A., Giallongo, E., Grazian, A., Salimbeni, S. ApJ 647, 753
 Monaco, P., Salucci, P., Danese, L. 2000, MNRAS 311, 279
 Monaco, P., & Fontanot, F. 2005, MNRAS 359, 283
 Monaco, P., Fontanot, F. & Taffoni, G. 2006, MNRAS accepted (astro-ph/0610805)
 Natali, F., Giallongo, E., Cristiani, S., & La Franca, F. 1998 AJ 115, 397
 Norman, C., Hasinger, G., Giacconi, R. et al. 2002, ApJ 571, 218
 Richards, G. T., Fan, X., Newberg, H.J. et al. 2002, AJ 123, 2945
 Richards, G. T., Croom, S.M., Anderson, S.F. et al. 2005, MNRAS 360, 839
 Richards, G. T., Strauss, M.A., Fan, X. et al. 2006, AJ 131, 2766
 Schneider, D. P., Hall, P.B., Richards, G. T. et al. 2005, AJ 130, 367

- Steffen, A.T., Strateva, I., Brandt, W.N., et al. 2006, ApJ 131, 2826
Szokoly, G. P., Bergeron, J., Hasinger, G. et al. 2004, ApJS 155, 271
Vanzella, E., Cristiani, S., Dickinson, M. et al. 2006, A&A 454, 423